参考著作No.12

KSCE Journal of Civil Engineering
July 2018, Volume 22, Issue 7, pp 2241–2255 | Cite as

Scour Depth Evaluation of a Bridge with a Complex Pier Foundation

Authors Authors and affiliations

Kuo-Wei Liao, Yasunori Muto, Jhe-Yu Lin

参考著作No.12

KSCE Journal of Civil Engineering (2018) 22(7):2241-2255

DOI 10.1007/s12205-017-1769-1

Geotechnical Engineering

pISSN 1226-7988, eISSN 1976-3808
www.springer.com/12205

Scour Depth Evaluation of a Bridge with a Complex Pier Foundation

Kuo-Wei Liao*, Yasunori Muto, and Jhe-Yu Lin*****

Received October 30, 2016/Revised June 30, 2017/Accepted July 23, 2017/Published Online October 12, 2017

Abstract

A scour depth prediction formula for a river bridge is established using experimental data in which the effects of the pier, pile-cap and pile group are considered. More than 170 experimental data entries, including different pier structural sizes, flow depths and soil covering depths, are collected and verified by existing formulae, which failed to deliver a promising prediction. A machine learning prediction model was then developed to enhance the accuracy. For application purpose, a sequential quadratic programming optimization was adopted to construct an explicit prediction formula. The MAPE was significantly improved from 102.8 to 28.9. The results indicate that the proposed formula can simultaneously satisfy the requirements of accuracy and simplicity. The proposed formula has the advantages of being conceptually consistent with observed scour behaviors and provides a solid scour depth prediction, which is an important and critical step in the bridge safety evaluation if floods are considered.

Keywords: *scour, flood, complicated foundation, optimization, machine learning*

1. Introduction

The rivers in Taiwan mostly start at the mountain areas at an altitude above 3000 m and are often shorter than 200 m. The rivers and streams are often steep with rapid currents. In addition, due to the uneven rainfall distribution over space and time, the rainfall at wet and dry periods varies significantly such that rivers are likely to cause floods during the wet periods, leading to river bed scouring and debris flow, etc. Bridges are important infrastructures for traffic connecting two shores of rivers. However, bridge structures built in rivers often block the river courses, changing the flow conditions and leading to local scouring of the piers. Consequently, the river bridge foundations are exposed and damaged, endangering the lives and safety of road users. According to Andrić and Lu (2016), the primary reason for bridge damage in the U.S. is related to flooding. According to a report of Construction Research Institute in Taiwan, bridges in Taiwan also have the same trend. Therefore, bridge safety evaluation against floods has attracted substantial attention of many scholars and engineers. River bed scouring can mainly be divided into the following three types: general scour, contraction scour and local scour. The content of this paper focuses on local scour only, which is generally considered to be the most important part for bridge safety. Most of the pier scour research has focused on the scour with uniform piers (Salim and Jones, 1996), which had not considered the impacts of the pile-caps and pile groups on the scour depth. A non-uniform pier is one for which the cross-sectional dimension varies over the length of the pier. In the early engineering practice in Taiwan, the scour formula with a uniform foundation was often used. In reality, most of the bridges lack uniform piers such that the applicability of the uniform pier formulae is inadequate. Thus, this study focuses on building an accurate non-uniform (complicated foundation) scour formula. For scours of non-uniform piers, many important impact factors should be considered, such as the soil covering depth, pier width, pile-cap width, flow velocity, riverbed materials, scouring period and so on. The factors affecting the pier scour can be categorized as the pier geometry, flow property, material characteristic at the riverbed and scour lag, etc., which are described in detail below:

The influencing factors include the pier width perpendicular to the flow direction (b_c), flow attack angle (θ), pile-cap width (b_{pc}), and soil covering height (level of the top surface of the pile cap below the surrounding bed level, Y). When the pier width (b_c) increases, the scour depth (d_s) also increases. If the piers are aligned with flow, the pier length (L) has no obvious impact on the scour depth (d_s). If a uniformly circular pier is considered, the flow attack angle (θ) and pier length (L) have no influence on the scour depth (d_s). Imamoto and Ohtoshi (1987) used the scour hole geometric similarity characteristic method while considering the horseshoe vortex and sediment transport to simulate scouring of non-uniform piers. They found that when the non-uniform ratio is greater (such as the difference between the pier width, b_c and pile-cap width, b_{pc}), the pier scour depth is smaller. Melville and Raudkivi (1996) divided non-uniform piers into the following

*Associate Professor, Dept. of Bioenvironmental Systems Engineering, National Taiwan University, Taiwan (Corresponding Author, E-mail: liaokuo-wei@gmail.com)
**Professor, Dept. of Civil & Environmental Engineering, Tokushima University, Tokushima, Japan (E-mail: muto_yas@ce.tokushima-u.ac.jp)
***Former Research Assistant, Veterans Affairs Council, Taiwan (E-mail: lcd2010mia@gmail.com)

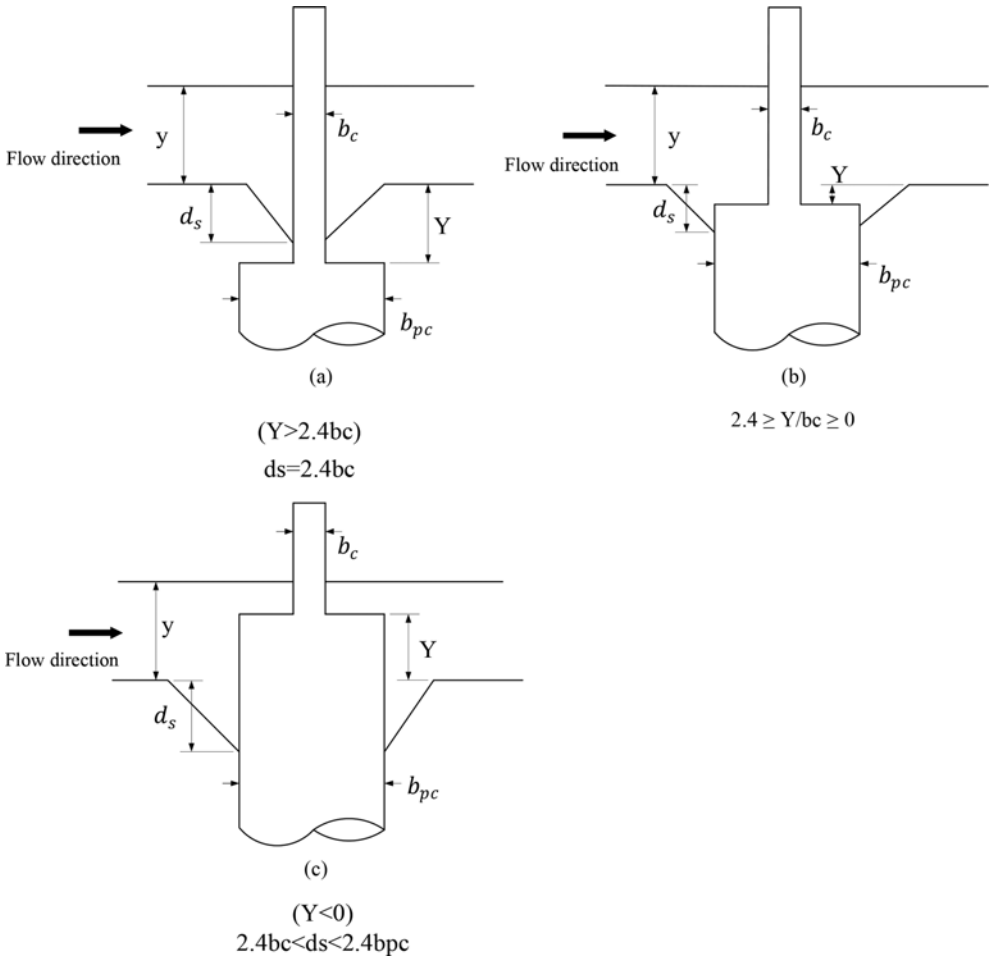

Fig. 1. Configurations of Non-uniform Circular Piers (Melville and Raudkivi, 1996): (a) Zone 1, (b) Zone 2, (c) Zone 3

3 configurations based on the soil covering depth (Y): (1) pile-cap is below the bottom of the scour hole (Zone 1, $Y/b_c > 2.4$), (2) pile-cap top is within the scour hole (Zone 2, $2.4 \geq Y/b_c \geq 0$), and (3) pile-cap top is above the bed level (Zone 3, $Y/b_c < 0$), as shown in Fig. 1. Compared to the scour results of a uniform pier, their experimental results indicated that Zone 1 does not affect the scour, Zone 2 reduces the scour and Zone 3 increases the scour depth.

The influential factors include the fluid density (ρ), flow velocity (V), flow depth (y), and gravitation acceleration (g). Depending on the magnitude of velocity (V), the scour can be divided into two types, clear-water and live-bed scour (Raudkivi, 1986). In the case of clear-water scouring, the scour depth increases as a function of the flow velocity without sediment movement. In the case of live-bed scouring, because the flow velocity exceeds the critical velocity of sediment movement (Vc), sediment transports across the bed surface, complicating the scour status (Wang *et al.*, 2016). As the velocity exceeds the threshold velocity (Vc), the scour depth first decreases and then increases to a second peak (Melville, 2008). As a result, average scour depth of the live-bed scour is smaller than that of the clear-water scour depth (Melville and Coleman, 2000). Because of this, the clear-water scour depth is often adopted as the primary factor for bridge safety evaluation. In this study, in addition to considering the existing data on the clear-water scour, 4 clear-water scours are conducted in the Hydrotech Research Institute of the National Taiwan University, and all of the data are used to build the proposed formula.

The flow depth (y) is typically standardized based on the pier width (b_c), meaning that the value of (y/b_c) is used to measure its impact on the scour depth. When the value of y/b_c is greater, the impact on the scour depth is greater and vice versa. Raudkivi and Ettema (1983) reported that if the value of y/b_c is greater than 3~4, the impact of the change of flow depth on the scour depth can be ignored (i.e., deep-water). The Reynolds number is often considered as one of the factors impacting the scour depth, as shown in Eq. (1).

$$d_{se} = 0.00073 \times R^{0.619} \tag{1}$$

where d_{se} refers to the equilibrium scour depth and R refers to the Reynolds number. According to Eq. (1), the scour depth increases along with increases in the Reynolds number. However, once it is increased to a particular value, the scour depth drops and the maximum value obtained at that particular value is the equilibrium

scour depth. Compared to the Reynolds number, the Froude number, a dimensionless parameter representing the relative importance of the inertia and gravity effects, is often considered as a more important factor affecting the scour depth (Jain and Fisher, 1980). Hydraulic Engineering Circular No. 18 (HEC-18, 2012) is another example in which the Froude number, instead of Reynolds number, is incorporated into the prediction formula, as shown in Eq. (2)

$$\frac{d_s}{y} = \left[2.0 K_1 K_2 K_3 \left(\frac{b_c}{y} \right)^{0.65} \left(\frac{V}{\sqrt{gy}} \right)^{0.43} \right] \quad (2)$$

wherein d_s is the scour depth; K_1 refers to the pier shape correction factor; K_2 refers to the correction coefficient for the angle of attack of flow; K_3 refers to the river bed material correction coefficient; b_c refers to the pier width perpendicular to the flow; and $\frac{v}{\sqrt{gy}}$ refers to the Froude number (Fr).

The influencing factors include the median grain size (d_{50}), river bed material standard deviation (σ_g), river bed material density (ρ_s), critical velocity of sediment movement (V_c) and so on. When the river bed material grain size is greater, the scour resistance is increased, resulting in a smaller local scour depth and vice versa. For example, Raudkivi and Ettema (1977) showed that when $b_c/d_{50} > 50$, classified as the fine grain river bed, the scour depth decreases along with decreasing b_c/d_{50}. In addition to the size of the bed material, its roughness also affects the local scour depth through the critical velocity of sediment movement (V_c). When the river bed material grain size distribution is uneven, the armoring phenomena at the surface of the river bed material surface is formulated such that critical velocity of sediment movement is increased, decreasing the scour depth. Raudkivi and Ettema (1977) reported that during the clear-water scour, the local scour depth is significantly reduced along with an increase in the σ_g. When σ_g is greater than 1.3, the armoring phenomena are initiated.

The equilibrium of the scour depth (d_{se}) was mainly affected by the effect of the fluid flow and sediment transportation. The scour depth could reach 50~80% of the equilibrium scour depth by approximately 10% of the equilibrium scour time. Melville and Chiew (1999) suggested that when the change in the scour depth within 24 hours does not reach 5% of the pier width (b_c), the scour depth is the equilibrium scour depth (d_{se}), and its corresponding time refers to the equilibrium scour time (t_e). As shown in Fig. 2, compared to the live-bed scour, the time for the clear-water scour to reach equilibrium is slower. However, the live-bed scour would generate irregular vibrations due to the continuous transport of the river bed sediments. The equilibrium scour time (t_e) is also affected by the flow velocity, as shown in Fig. 3.

Many scholars have proposed approaches to calculate the scour depth for a pier with a non-uniform width. Among these, HEC-18 (2012) and Melville and Coleman (2000) comprehensively include the aforementioned scour factors and are more popular. As a result, they are selected as the baseline calculation in this study. HEC-18 divides the non-uniform piers into three parts (pier, pile-cap and pile group) and uses the linear superposition to predict the scour depth. Melville and Coleman (2000) take advantage of the existing formula of a uniform pier such that it would be required to obtain the equivalent pier width (b_e) for a non-uniform pier prior to further calculation. This study first collects relevant experimental data, including data documented in the literature and new experiments. Sensitivity analysis is conducted on the experimental data to determine the important impact factors, which is followed by use of the least-square support vector machine (LS-SVM) to calculate the scour depth. Compared to the previous calculation methods (HEC-18 and Melville and Coleman, 2000), LS-SVM significantly increases the prediction accuracy. However, engineers are relatively more familiar with the utilization of formulae during the design compared to artificial intelligence (such as LS-SVM). As a result, the formula proposed by Melville and Coleman (2000) is further used with the optimization method to find the relative weight of each impact factor and enhance the prediction accuracy. The result indicates that the accuracy significantly increases, although it is slightly less than that of LS-SVM. The following provides descriptions on the existing scour depth calculation method, the artificial intelligence method (LS-SVM) adopted here, the calculation procedure of the proposed formula and the results of the analysis on the collected data.

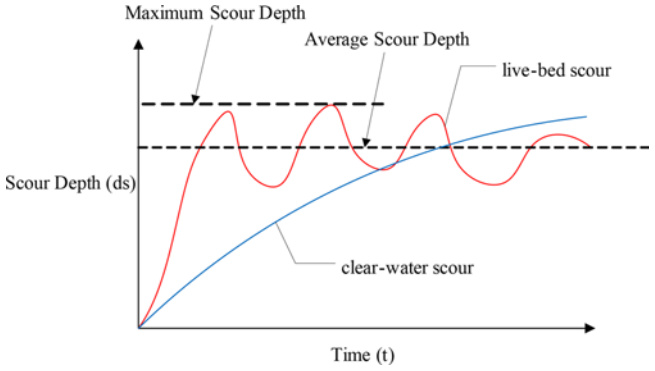

Fig. 2. Schematic View of the Relationship between the Scour Depth and Time (Raudkivi, 1986)

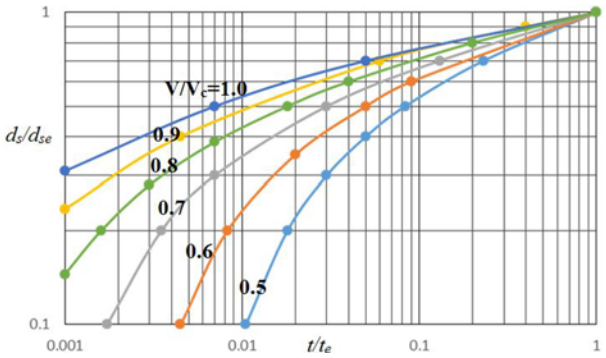

Fig. 3. Relationship between the Scour Depth (d_s), eQuilibrium Scour Time (t_e) and Flow Velocity (V/V_c)

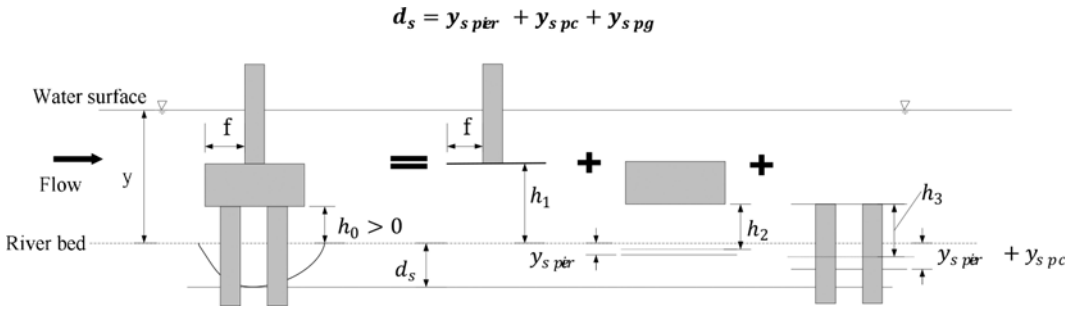

Fig. 4. Schematic View of HEC-18 Non-uniform Pier Scour Calculation

2. Material and Methods

Although the current study develops a method to predict the scour depth based on the following existing methods, please note other approaches are available. For example, Najafzadeh and Azamathulla (2013) proposed a quadratic polynomial of Group Method of Data Handling (GMDH) network, improved by the back propagation algorithm, to predict scour depth around bridge piers. Najafzadeh *et al.* (2016) integrated Gene-expression Programming (GEP), Evolutionary Polynomial Regression (EPR), and Model Tree (MT) to predict the scour depth around bridge piers with debris effects.

2.1 Existing Method - the HEC-18 Approach

Equation (2) refers to the scour formula proposed by HEC-18 for a uniform pier. For the foundation with a non-uniform width, HEC-18 divides the pier structure into three parts, as shown in Fig. 4, and these three parts are the pier ($y_{s\,pier}$), pile-cap ($y_{s\,pc}$) and pile group ($y_{s\,pg}$). The calculation of the scour depth involves a step-by-step process, and the amount of scouring for the pile-cap ($y_{s\,pc}$) and pile group ($y_{s\,pg}$) need to take into account the impacts of the former (such as the pier part) to provide an updated soil covering height (h_1, h_2, and h_3), followed by re-calculating the equivalent flow velocity and equivalent pier width perpendicular to the flow for each part. After computing the three parts separately, the sum of the three parts would then yield the predicted scour depth, as shown in Eq. (3). Fig. 4 demonstrates that HEC-18 uses h_0 to show the soil covering height; h_0 is defined as the height of the pile cap above the bed at beginning of computation. This h_0 is opposite from the Y value, and the relationship between the two can be expressed in Eq. (4).

$$d_s = y_{s\,pier} + y_{s\,pc} + y_{s\,pg} \tag{3}$$

$$\begin{aligned} h_0 &= -(Y+T) \\ h_1 &= h_0 + T \end{aligned} \tag{4}$$

When HEC-18 is used, the Y values need to be utilized to determine the required formula, which can be divided into two scenarios, Y > 0 and Y < 0. The case with Y > 0 refers to (1), (2) and (3) in Fig. 5. The case with Y < 0 refers to (4), (5), (6) and (7) in Fig. 5. When Y > 0, the bridge foundation is considered to be of a uniform pier, and the scour depth calculation is similar to Eq. (2), as shown in Eq. (5):

$$\frac{d_s}{y} = \left[2.0 K_1 K_2 K_3 K_w \left(\frac{b_c}{y} \right)^{0.65} \left(\frac{V_1}{\sqrt{gy}} \right)^{0.43} \right] \tag{5}$$

where V_1 refers to the approach velocity used at the beginning of computations, and K_w refers to the correction factor for wide piers with shallow flow.

The case with Y < 0, it can be further classified into two scenarios, Y > -T or Y < -T. When Y > -T, referring to (4) in Fig. 5, the impact of the pile group does not need to be considered, but the scour depth needs to consider $y_{s\,pier}$ and $y_{s\,pc}$. When computing the $y_{s\,pier}$, because the pile-cap is already exposed in the water, it would have a protruding value (f, as shown in Fig. 4), and such an f value (distance between front edge of pile-cap or footing and pie) would cause a shielding effect. HEC-18 uses $K_{h\,pier}$ to consider such an effect, as expressed in Eq. (6). From Eq. (6), it can be learned that $0 < K_{h\,pier} < 1$, meaning that when Y > -T, the scour depth of the pier cannot be greater than the scour value of the uniform pier and it is not possible to be a negative value. At this time, the scour depth ($y_{s\,pier}$) caused by the pier part can be calculated via Eq. (7). Whereas the scour depth ($y_{s\,pc}$) caused by the pile-cap part can be calculated via Eq. (8).

$$\begin{aligned} K_{h\,pier} = &\left(0.04075 - 0.0669 \frac{f}{b_c} \right) - \left(0.4271 - 0.0778 \frac{f}{b_c} \right) \left(\frac{h_1}{b_c} \right) + \\ &\left(0.1615 - 0.0455 \frac{f}{b_c} \right) \left(\frac{h_1}{b_c} \right)^2 - \left(0.0269 - 0.012 \frac{f}{b_c} \right) \left(\frac{h_1}{b_c} \right)^3 \end{aligned} \tag{6}$$

$$\frac{y_{s\,pier}}{y} = K_{h\,pier} \left[2.0 K_1 K_2 K_3 K_w \left(\frac{b_c}{y} \right)^{0.65} \left(\frac{V_1}{\sqrt{gy}} \right)^{0.43} \right] \tag{7}$$

$$\frac{y_{s\,pc}}{y_f} = \left[2.0 K_1 K_2 K_3 K_w \left(\frac{b_{pc}}{y_f} \right)^{0.65} \left(\frac{V_f}{\sqrt{g y_f}} \right)^{0.43} \right] \tag{8}$$

where b_{pc} refers to the width of the original pile-cap, $y_f = h_1 + y_{s\,pier}/2$ is the distance from the bed to the top of the footing, and V_f is the average velocity in the flow zone below the top of the footing and can be calculated as follows.

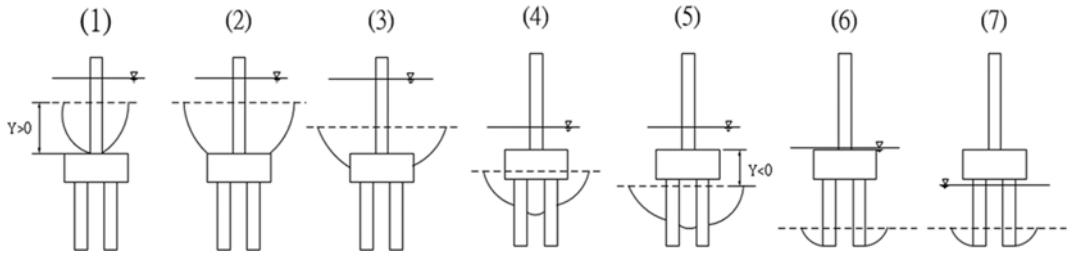

Fig. 5. Schematic View of Various Scour Scenarios

$$\frac{V_f}{V_2}=\frac{Ln\left(10.93\frac{y_f}{K_s}+1\right)}{Ln\left(10.93\frac{y_2}{K_s}+1\right)} \tag{9}$$

where $V_2 = V_1(y_1/y_2)$ is the average adjusted velocity in the vertical flow approaching the pier, V_1 is the original approach velocity at the beginning of the computations, y_1 is the original flow depth at the beginning of the computations before scouring, $y_2 = y_1 + y_{s\,pier}/2$ = the adjusted flow depth, and K_s is the grain roughness of the bed.

For the case of Y < -T, referring to (5), (6) and (7) in Fig. 5, the scour depth calculation needs to consider $y_{s\,pier}$, $y_{s\,pc}$ and $y_{s\,pg}$. The calculation of $y_{s\,pier}$ is similar to the above, and Eq. (7) is used for the calculation; as for the scour depth ($y_{s\,pc}$) caused by the pile-cap part, the approach is similar to Eq. (8) but with modification because the pile-cap part is completely exposed in the water. Consequently, when Y < -T, $y_{s\,pc}$ is calculated via Eq. (10). As for the sour depth ($y_{s\,pg}$) caused by the pile group art, it is calculated via Eq. (11).

$$\frac{y_{s\,pc}}{y_f}=\left[2.0K_1K_2K_3K_w\left(\frac{b^*_{pc}}{y_f}\right)^{0.65}\left(\frac{V_f}{\sqrt{gy_f}}\right)^{0.43}\right] \tag{10}$$

$$\frac{y_{s\,pg}}{y_3}=K_{h\,pg}\left[2.0K_1K_3\left(\frac{b^*_{pg}}{y_3}\right)^{0.65}\left(\frac{V_3}{\sqrt{gy_3}}\right)^{0.43}\right] \tag{11}$$

where b^*_{pc} is the width of the equivalent pier and can be calculated using Eq. (12); $y_3 = y_1 + y_{s\,pier}/2 + y_{s\,cap}/2$ = the adjusted flow depth; $K_{h\,pg}$ is the pile group height factor; b^*_{pg} is an equivalent pile group width that considers non-overlapping projected widths of piles, pile spacing, pile alignment and skewed or staggered pile groups; and $V_3 = V_1(y_1/y_3)$ = the average adjusted velocity.

$$\frac{b^*_{pc}}{b_{pc}}=Exp\left[-2.705+0.51Ln\left(\frac{T}{y_2}\right)-2.783\left(\frac{h_2}{y_2}\right)^3+1.751/Exp\left(\frac{h_2}{y_2}\right)\right] \tag{12}$$

where $h_2 = h_0 + y_{s\,pier}/2$.

2.2 Existing Method - the Method of Ataie-Ashtiani *et al.* (2010)

HEC-18 considers the scour depth in the following three computation methods: (1) only the pier is considered, (2) the pier and pile-cap are considered, and (3) three parts of the pier, pile-cap and pile group are considered. Based on the experimental results, Ataie-Ashtiani B *et al.* (2010) claimed that the estimated scour depth of the pile-cap part is overly conservative and proposed a modification as expressed in Eq. (13).

$$d_s = K_A y_{s\,pier} + K_B y_{s\,pc} \tag{13}$$

where K_A refers to the correction coefficient of the pier part, as shown in Eq. (14). K_B refers to the correction coefficient of the pile-cap part, as shown in Eq. (15).

$$\begin{cases} K_A = 0.4\left(2.5-\frac{f}{b_c}\right) & \text{if } \frac{f}{b_c}\le 2.5 \\ K_A = 0 & \text{otherwise} \end{cases} \tag{14}$$

$$K_B=\left(\frac{b_{pc}}{y_{new}}\right)^{0.1} \tag{15}$$

where f refers to the distance between front edge of the pile-cap or footing and pie and y_{new} refers to the corrected water depth = $y + K_A y_{s\,pier}$.

2.3 Existing Method – the Melville & Coleman's Approach

Melville and Coleman (2000) proposed a prediction formula for the scour depth of complicated foundation, and the calculation method is expressed in Eq. (16).

$$d_s = K_{yb}K_sK_\theta K_1K_tK_d \tag{16}$$

where K_{yb} = water depth – bridge shape impact factor is as expressed in Eq. (17); K_s = pier shape correction factor is as expressed in Eq. (18); K_θ = correction coefficient of the angle of attack of flow, as expressed in Eq. (19); K_I = flow intensity correction coefficient, as expressed in Eq. (20); K_t = time factor correction coefficient, as expressed in Eq. (21); and K_d = river bed material characteristic correction coefficient, as expressed in Eq. (22).

$$\begin{cases} K_{yb}=2.4b_e & \frac{b_e}{y}<0.7 \\ K_{yb}=2\sqrt{yb_e} & 0.7<\frac{b_e}{y}<5 \\ K_{yb}=4.5y & \frac{b_e}{y}>5 \end{cases} \tag{17}$$

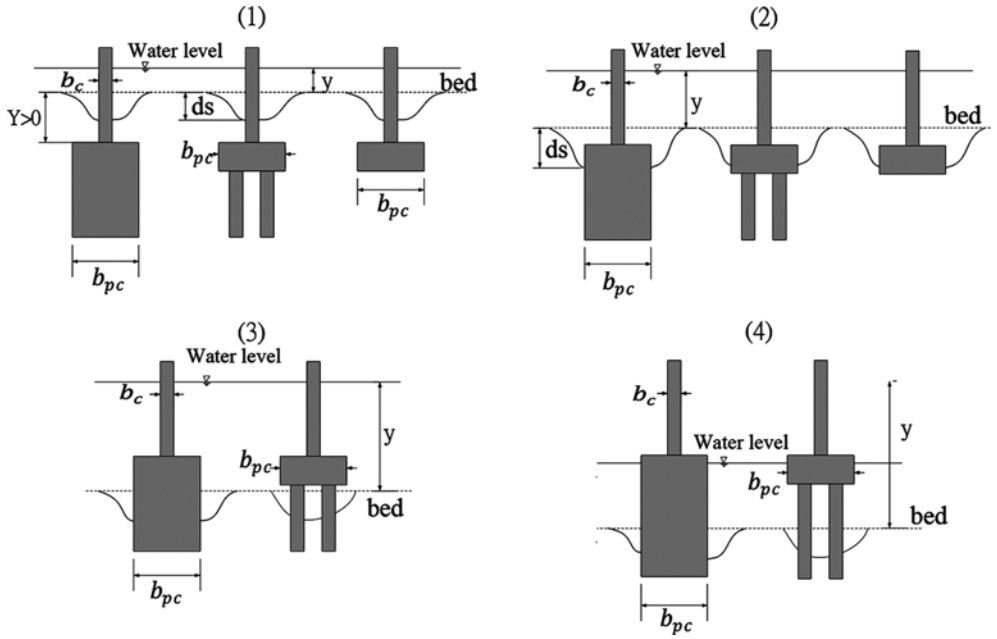

Fig. 6. Calculation of Equivalent Width Perpendicular to the Flow under four Different Types of Scour Cases

where b_e refers to the equivalent pier width perpendicular to the flow, and Eq. (17) suggests that when the flow depth $y/b_e > 1.429$ (referring to $b_e/y < 0.7$), the local scour depth of the pier is approximately 2.4 times the equivalent pier width (b_e). When the flow depth $y/b_e < 0.2$ (referring to $b_e/y > 5$), the scour depth is only related to the water depth, which is approximately 4.5 times the water depth. When the water depth is between 0.2 and 1.429, the equivalent pier width (b_e) and water depth both affect the local depth scour of the pier.

$$\begin{cases} K_s = 0.9 & \text{sharp nosed shape} \\ K_s = 1.0 & \text{circular, round nosed and group of cylinder} \\ K_s = 1.1 & \text{squared nosed shape} \end{cases} \tag{18}$$

Equation (18) indicates that K_s is approximately between 0.9~1.1, and this range is close to the corrected range proposed by Raudkivi (1986). Raudkivi (1986) proposed that the impact of the pier shape on the pier scour depth was far less than the impact of the flow attack angle, and the range of the pier shape correction factor should be between 0.7~1.2.

$$K_\theta = \left(\frac{L}{b_e} sin\theta + cos\theta \right)^{0.65} \tag{19}$$

where L refers to the pier length and q refers to the angle of attack of the flow. In general, excluding circular column piers ($K_\theta = 1$), the equivalent pier width (b_e) would increase along with the increase in the angle of attack of the flow, as indicated in Eq. (19).

$$\begin{cases} K_I = \dfrac{V-(V_a-V_c)}{V_c} & \text{if } \dfrac{V-(V_a-V_c)}{V_c} < 1 \\ K_I = 1.0 & \text{otherwise} \end{cases} \tag{20}$$

where V_a refers to the non-uniform critical velocity of sediment movement.

$$K_t = \exp\left\{ -0.03 \left| \frac{V}{V_c} \ln\left(\frac{t}{t_e} \right) \right|^{1.6} \right\} \tag{21}$$

$$\begin{cases} K_d = 0.57 \log\left(2.24 \dfrac{b_e}{d_{50}} \right) & \dfrac{b_e}{d_{50}} \le 25 \\ K_d = 1 & \text{otherwise} \end{cases} \tag{22}$$

where d_{50} refers to the median grain size.

From the above computation process, it can be learned that in Melville and Coleman's approach, the equivalent pier width (b_e) plays a key role. Additionally, when the water depth, river bed location and pier type are considered, b_e may be slightly different, which can mainly be classified into four cases (as shown in Fig. 6). The scenario of Case 1 ($Y > b_{pc}$ where b_{pc} refers to the pile-cap width perpendicular to the flow) and the impacts of the pile-cap and pile group can be ignored. In this case, $b_e = b_c$. The values of b_e for Case 2 ($Y \le b_{pc}$ and $Y > 0$) and Case 3 ($Y \le 0$ and $-Y < y$) need to consider the width perpendicular to the flow for both the pier and pile-cap. During the calculation of the scour depth in Case 4, b_e is assumed to be b_{pc}. The four types of cases, after organization, can be expressed in Eq. (23).

$$\begin{cases} b_e = b_c & Y > b_{pc} \\ b_e = b\left(\dfrac{y+Y}{y+b_{pc}} \right) + b_{pc}\left(\dfrac{b_{pc}-Y}{y+b_{pc}} \right) & b_{pc} \ge Y \ge 0 \\ b_e = b\left(\dfrac{y+Y}{y+b_{pc}} \right) + b_{pc}\left(\dfrac{b_{pc}-Y}{y+b_{pc}} \right) & 0 \ge Y \ge -y \\ b_e = b_{pc} & -Y > y \end{cases} \tag{23}$$

From Eq. (23), it can be learned that for Cases 2 and 3 in Melville and Coleman's approach, the calculations of b_e are identical.

2.4 The Proposed Calculations for the Scour Depth of a Bridge with a Complex Pier

Two alternative approaches for calculating the scour depth are proposed. The first method uses the machine learning theory, and the second method uses the sequential quadratic programming to find the optimal coefficients in the proposed formula, as described below:

2.4.1 Using Machine Learning Technique

In addition to the existing formulae introduced earlier, Artificial Neural Networks (ANNs) or Support Vector Machines (SVMs) are potential tools that can be used to build a prediction model of scour depth. ANNs have been successfully applied to many civil engineering problems, such as predicting the bearing capacity of strip footing (Kuo *et al.*, 2009), analyzing the slope stability analysis (Cho, 2009), predicting the rock fragmentation due to blasting (Bahrami *et al*., 2011), predicting the groutibility of microfine cements in permeation grouting (Liao *et al*., 2011) and predicting the scour depth (Hosseini *et al.,* 2016; Lashkar-Ara *et al.*, 2016). The SVM is another useful technique for data classification and regression. Constructing a SVM is often considered to be easier than building an ANN model. SVMs also have been applied to many engineering problems, such as predicting the blast-induced ground vibration (Khandelwal, 2011), identifying the lateral flow occurrence (Lee and Kim, 2010), predicting the side weir discharge coefficient (Azamathulla *et al*., 2016), forecasting head loss on cascade weir (Haghiabi *et al*., 2016) and detecting the rusted area in a steel bridge (Liao and Lee, 2016). Although the SVM has been recognized a powerful tool, only few of researches has investigated its suitability in scour depth prediction (). Thus, SVM is chosen as one of the proposed approaches to calculate the scour depth for a bridge with a complex pier.

A standard SVM, as described in Eq. (24), solves a nonlinear classification problem by means of convex Quadratic Programs (QP).

$$\underset{w,b,\xi}{\text{minimize}}\ \frac{1}{2}w^T w + c\sum_{k=1}^{N}\xi_k$$
$$\text{Subject to}\ \begin{cases} y_k\left(w^T K(x_i)+b\right) \ge 1-\xi_k \\ \xi_k \ge 0,\ i=1,2,...,N \end{cases} \tag{24}$$

where w is a normal vector to the hyper-plane; c is a real positive constant; and ξ_k is the slack variable. If $\xi_k > 1$, the k-th inequality becomes violated compared to the inequality from the linearly separable case. y_k is the class; $[w^T K(x_i) + b]$ is the classifier; N is the number of data; and K is the kernel function. In the current study, the Gaussian Radial Basis Function (RBF) kernel is used, as shown in Eq. (25).

$$K(X, X_i) = e^{-\sigma(\|X-X_i\|)^2} \tag{25}$$

where X is the input vector, σ is the kernel function parameter; and X_i are the support vectors. LS-SVM (Suykens *et al.*, 2002), instead of solving the QP problem, solves a set of linear equations by modifying the standard SVM, as described in Eq. (26).

$$\min\ \frac{1}{2}w^T w + \frac{\gamma}{2}\sum_{k=1}^{N}e_k^2$$
$$\text{s.t.}\ y_k(w\cdot K(x_k)+b) = 1-e_k,\ k=1,...,\text{n} \tag{26}$$

where γ is a constant number and ε is the error variable. Compared to the standard SVM, there are two modifications leading to solving a set of linear equations. First, instead of inequality constraints, the LS-SVM uses equality constraints. Second, the error variable is a squared loss function.

Because the input data play an important role in the LS-SVM, the selections of input parameters are described below. Two LS-SVM models are developed. The inputs of the first and second models are approximately considered as HEC-RAS-based and Melville and Coleman-based LS-SVMs. Based on the aforementioned introduction and Buckingham π theorem, the results of the dimensional analysis for the HEC-RAS and Melville & Coleman approaches can be described as shown in Eqs. (27) and (28).

$$\frac{d_s}{b_c} = f\left(\frac{V}{\sqrt{gy}}, \frac{y}{b_c}, \frac{D_{50}}{b_c}, \sigma_g, \frac{V}{V_c}, \frac{b_{pc}}{b_c}, \frac{b_{pg}}{b_c}, \frac{Y}{b_c}, \frac{f}{b_c}, \frac{L}{b_c}\right) \tag{27}$$

$$\frac{d_s}{b_e} = f\left(\frac{V}{V_C}, \frac{y}{b_c}, \frac{D_{50}}{b_e}, \sigma_g, \frac{Y}{b_e}, \frac{L}{b_e}\right) \tag{28}$$

Although the two sets of input factors are similar, differences between them are noticeable. For example, the basic dimensions of HEC-RAS and Melville & Coleman are b_c and b_e, respectively. Furthermore, the widths of the pile-cap and pile groups are explicitly considered in the HEC-RAS-based LS-SVM model. Please note that factors displayed in Eqs. (27) and (28) only include the available factors in the collected experiment data. Table 1 displays the data range used for developing LS-SVM in the current study.

2.4.2 Using Formula-based Approach

It is recognized that neither ANNs nor SVMs provide a specific formula for engineers, although they have the potential to deliver a promising prediction (Huang *et al*., 2013). The concept and

Table 1. Data Range Used for Developing LS-SVM

	y	b_c	b_{pc}	L_u	Y	V/V_c	d_{50}	σ_g	d_s
Max.	0.6	0.1524	0.3694	2.78	0.205	1.183206	0.001	1.3	0.338328
Min.	0	0	0	0	-0.67	0	0	0	0

operation of an ANN or an SVM model is a black box for some practical engineers. On the other hand, an explicit formula is often used in civil/hydraulic engineering. Thus, one of the goals in this study is aimed to develop a formula with a similar format to that of existing formulae that provides an analogous evaluation procedure but with higher accuracy for predicting scour depth in a bridge with a complex pier. Details are provided below.

Although the concept of superposition used in HEC-18 is straightforward, updating several parameters in different cases complicates the prediction process (Section 2.1). Melville and Coleman (2000) treats the pier as a single element resulting in a single formula, which is more suitable to the engineering application in practice. Therefore, the formula in Melville and Coleman (2000) is used as the basis to develop a new prediction formula. Eq. (23) describes the calculation of b_e; it is seen that b_e is basically interpolated using the two values of b_c and b_{pc}, as shown in Eq. (29).

$$b_e = A \times b_c + B \times b_{pc}, \text{ where } A + B = 1 \tag{29}$$

where A and B are the weights for b_c and b_{pc}, respectively, and the sum of the two weights is 1. According to the suggestion of Melville and Coleman (2000), A and B are functions of the flow depth (y), the level of the top surface of pile cap below surrounding bed level (Y) and the pile-cap width perpendicular to the flow (b_{pc}). Similarly, the optimization technique adopted here is used to obtain the function content of A and B, as described in Eq. (30).

$$b_e = \left(\frac{x_1 * y + x_2 * Y}{x_3 * y + x_4 * b_{pc}} \right) b_c + \left(\frac{x_5 * b_{pc} - x_6 * Y}{x_7 * y + x_8 * b_{pc}} \right) b_{pc} \tag{30}$$

where x_i refers to the coefficient to be determined. In addition to modifying the formula of b_e, from Eq. (23), it can be learned that the accuracy of the prediction of the scour depth also depends on the correct classification. For example, Eq. (23) classifies the formula into three types based on the value of Y (formulae for cases 2 and 3 are identical). However, according to the experimental results (e.g., Melville and Raudkivi, 1996), as shown in Fig. 7, it is obvious that the change in the scour depth near $Y = 0$ is extremely high such that it is not appropriate to use one identical formula (referring to Eq. (23)) for the calculations of the b_e values at two areas of Y that are greater than or smaller than 0. Therefore, calculation of b_e is classified into four different cases, as shown in Eq. (31), and the corresponding functions, such as f, g, h and k, are determined through the optimization method.

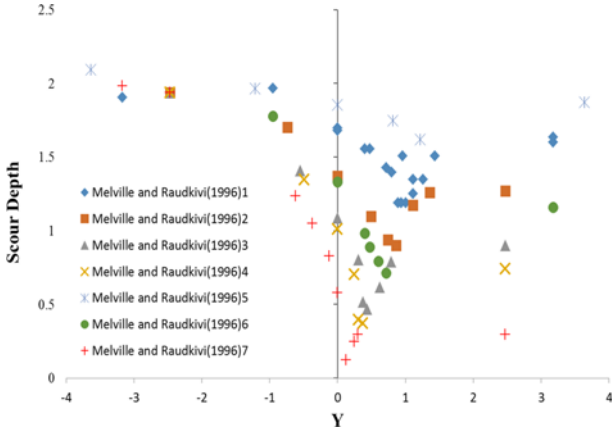

Fig. 7. Relationship between the Scour Depth (d_s) and Soil Covering Depth (Y)

$$\begin{cases} b_e = f(y, Y, b_c, b_{pc}) & Y > 2.4 b_c \\ b_e = g(y, Y, b_c, b_{pc}) & 2.4 b_c \geq Y \geq 0 \\ b_e = h(y, Y, b_c, b_{pc}) & 0 \geq Y \geq -y \\ b_e = k(y, Y, b_c, b_{pc}) & -Y > y \end{cases} \tag{31}$$

where the mathematical formulation of the optimization problem is described as follows.

$$\begin{aligned} &Min. \quad D_s - K_{yb} K_s K_\theta K_I K_t K_d \\ &s.t. \quad x_i, \; i = 1,2,...,8 \end{aligned} \tag{32}$$

where D_s refers to the scour depth obtained from the experiment, $K_{yb} K_s K_\theta K_I K_t K_d$ is the function of b_e, and the calculation of b_e is described in Eq. (30).

3. Results and Discussions

3.1 Data and Prediction Results using Existing Formulae

The scour depth experimental data collected in this study are shown in Table 2, including a total of 175 experimental data entries (comprising the four data entries of this research). The methods of Melville and Coleman (2000), HEC-18 (2012), Ataie-Ashtiani *et al.* (2010) and the proposed approaches including LS-SVM and formula-based method are used to perform the scour depth calculation. The calculated results are then compared with the experimental data to evaluate the accuracy of each method.

Figures 8-10 are the comparison charts of the analysis and experiment results conducted on the 175 data entries using the Melville and Coleman (2000), HEC-18 (2012) and Ataie-Ashtiani *et*

Table 2. Data Source and Information for the Collected Experiments

Sources	y/b_c	b_c/D_{50}	V/V_c	Y/b_c	f/b_c	T/b_c	b_{pc}/b_c
Sheppard and Renna (2005)	2	152	1.18	-0.2-1	0.1-0.5	0.2	-
Ataie-Ashtiani *et al.* (2010)	3.3-7.1	37-70	0.72-0.85	-8.2-3.2	0.42-0.68	1-1.45	0.38-0.73
Melville and Raudkivi (1996)	4.4-20	12-188	≈ 1	-20-2.5	0.11-3.55	-	-
Coleman (2005)	3.3-7.1	37-70	0.72-0.85	-8.2-3.2	0.42-0.68	1-1.45	0.38-0.73
Present study	3.57-4.18	76.5	0.53-0.91	0	0.454	0.954	0.68

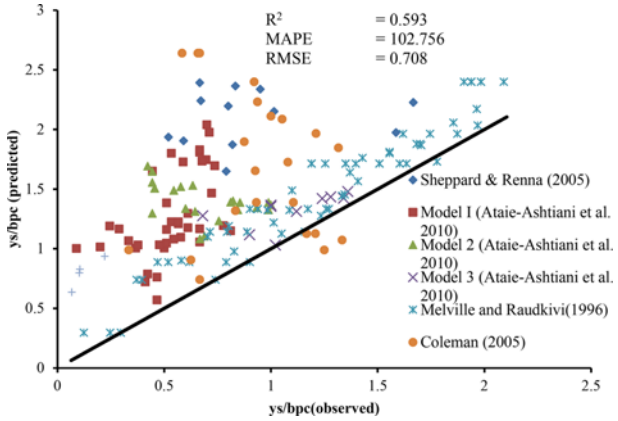

Fig. 8. Comparison between the Prediction Scour Values (Melville and Coleman, 2000) and Actual Scour Values

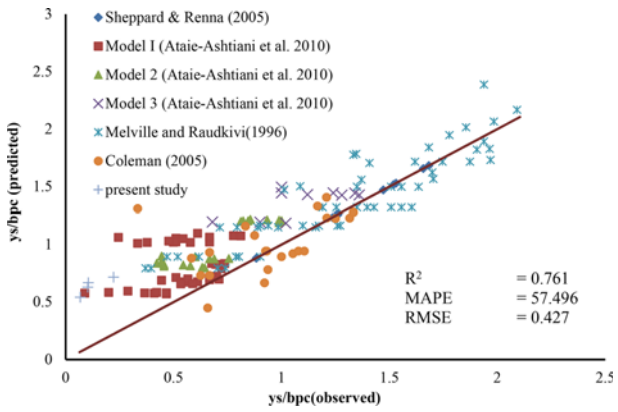

Fig. 9. Comparison between the Prediction Scour Values (HEC-18) and Actual Scour Values

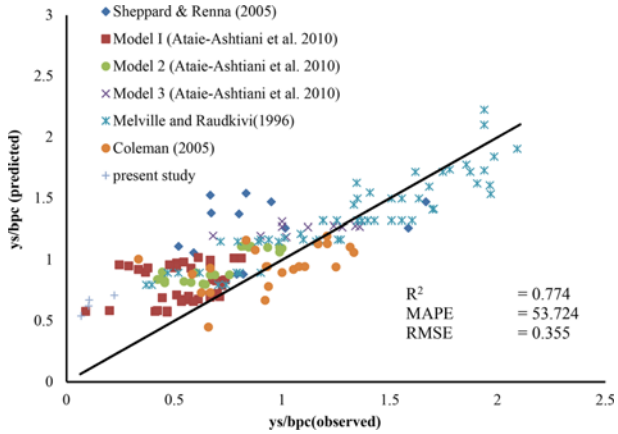

Fig. 10. Comparison between the Prediction Scour Values (Ataie-Ashtiani *et al.*, 2010) and Actual Scour Values

al. (2010) methods; wherein, the X axis refers to the actual scour and Y axis refers to the predicted scour depth. The prediction is considered accurate when the data points in Figs. 8-10 are on the reference line. Table 3 shows the accuracy evaluations on the aforementioned three methods. In Figs. 8-10 and Table 3, it can be seen that the prediction accuracy of the method of Melville and Coleman (2000) is relatively inaccurate. If the evaluation standard specified by Lewis (1982) is used (as shown in Table 4), the three calculation methods are all undesirable and are rated as inadequate.

Table 3. Error Evaluations of Scour Formulae

Calculation method	MAPE	RMSE
Melville& Coleman (2000)	102.7564	0.707848
HEC-18	57.4965	0.427707
Ataie-Ashtiani *et al.* (2010)	53.7245	0.354607

Table 4. MAPE Evaluation Ranking Table

MAPE (%)	Evaluation ranking
< 10	Most optimal
10 ~ 20	Excellent
20 ~ 50	Fair
> 50	Inadequate

3.2 Discussions for the Existing Formulae

From Fig. 8 and Table 3, it can be learned that for the method proposed by Melville *et al.* (2000), among the 175 data entries, only 8 data entries appear at the right side of the reference line, indicating that the overall prediction is too conservative. From Eq. (16), it is learned that the formula proposed by Melville *et al.* (2000) is mainly affected by six factors. Table 5 lists the numerical ranges of these factors that should be used as a basis for studying the source of the error. As shown in Table 5, the values of K_s, K_θ and K_d nearly have no impact on the predicted scour depth; for these, because no experiments consider the angle of attack of flow, the values of K_θ are all equal to 1. Consequently, the main source of error could be K_{yb}, K_I, and K_t. Wherein K_t is especially problematic because most of the experiments have extended the testing time to reduce the impact of time on the scour depth, and only an experimental value in all of the data of K_I is smaller than 0.7, while more than half of the values of the experimental result of K_I are equivalent to 1. Because of this, K_I and K_t should not be factors that cause MAPE > 100. In view of the above discussion, the key factor for error is K_{yb}. From Eq. (16), it is known that K_{yb} is greatly affected by the equivalent width perpendicular to the flow (b_e). Therefore, the formulation of b_e, as described in Section 3.2., is revised to enhance the prediction accuracy, as shown in Section 4.3.

Figure 9 and Table 3 show that the scour depth obtained from HEC-18 is of a smaller error compared to that of Melville *et al.* (2000). However, according to Table 4, the prediction result is

Table 5. Numerical Ranges of the Six Impact Factors of (Melville and Coleman, 2000)

Impact factor	Numerical range
K_{yb}	0.024 ~ 0.54
K_s	1.0 ~ 1.1
K_θ	1
K_I	0.53 ~ 1
K_t	0.76 ~ 1
K_d	1

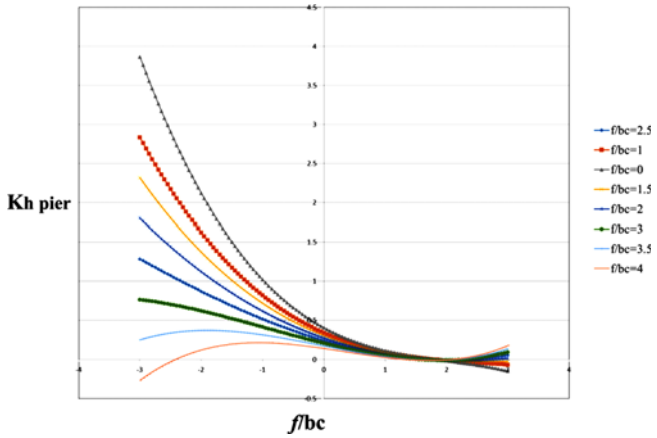

Fig. 11. Relationship between f/b_c and $K_{h\ pier}$

inadequate. $K_{h\,pier}$ is a possible factor that is described as follows. Parola *et al.* (1996) suggested that a rectangular pile-cap length would reduce the local scour depth. When the extension length of the pile-cap toward the upstream direction (f, as shown in Fig. 4) is approximately 2.3-2.5 of b_c (pier width perpendicular to the follow), it is able to effectively reduce the scour depth. In the collected data, the ratio of f/b_c is between 0.2~7.1. When the ratio f/b_c exceeds 2.5, the trend of $K_{h\,pier}$ (as shown in Fig. 11) does not follow the direction suggested by HEC-18 (Section 2.1, $0 < K_{h\,pier} < 1$, and it cannot be a negative value). When f/b_c is greater than 2.5, the applicability of the $K_{h\,pier}$, which was suggested by HEC-18 to take the effect of f/b_c, is questionable.

3.3 Prediction Results using the Proposed Methods

Table 6 shows results of using LS-SVM to predict the scour depth. The common 5-fold method is used to prevent overfitting of the data. In addition, to decrease overfitting, a total of 9 analyses of 5-fold are conducted, meaning that for each LS-SVM model, there are a total 45 prediction results. Table 6 shows the average value and Coefficient of Variation (COV) of the prediction result. According to Table 6, the results of MAPE are generally 25~27, which are within the reasonable range (Table 4). Compared to the existing formulae used, LS-SVM increases the accuracy by approximately 2~4 times. Regardless of whether it is MAPE or R^2, the two LS-SVM prediction results do not significantly differ from each other. By using MAPE as an example, there is only a difference of approximately 2%, which means that the two sets of different input parameters have relatively small impact on the LS-SVM results as well as that the input parameters considered by Melville and Coleman (2000) should yield prediction results that are similar to the ones of HEC-18. Because engineers often prefer the formula-based approach over a machine learning method, this study proposed an alternative approach and the results are described as follows. Table 7 provided an error comparison using different kernel functions, indicating that RBF is a better selection than the linear kernel. Please note that other kernel functions are available for the use in SVM, their performance investigation is important but is beyond the scope of current study.

Table 6. Accuracies of using LS-SVM to Predict the Scour Depth

Analysis method	MAPE (%)	R^2
Melville and Coleman-based LS-SVM	27.2 (0.31)*	0.79 (0.19)*
HEC-18-based LS-SVM	25.1 (0.28)*	0.84 (0.06)*

*the number inside the brackets refers to COV

Table 7. Accuracies of Melville and Coleman-based LS-SVM for different kernel functions

Kernel function	MAPE (%)	R^2
RBF	27.2 (0.31)*	0.79 (0.19)*
Linear	34.6 (0.02)*	0.62 (0.02)*

*the number inside the brackets refers to COV

The sequential quadratic programming from the MATLAB toolbox is used to solve the optimization problem described in Eq. (32). The objective of the optimization is to find 8 coefficients of the functions of f, g, h and k in Eq. (31); wherein when $Y > 2.4b_c$ it is typically recognized so that it is not scoured to the location of the pile-cap and so that the influence of pile-cap and pile groups can be ignored. Therefore, under such conditions, optimization is not performed, indicating that $f = b_c$ and $b_e = b_c$. Optimization results are described in Eqs. (33), (34) and (35).

$$\begin{cases} b_e = f(y,Y,b_c,b_{pc}) & Y > 2.4b_c \\ b_e = g(y,Y,b_c,b_{pc}) & 2.4b_c \geq Y \geq 0 \\ b_e = h(y,Y,b_c,b_{pc}) & 0 \geq Y \geq -y \\ b_e = k(y,Y,b_c,b_{pc}) & -Y > y \end{cases} \tag{33}$$

$$b_e = g(y,Y,b_c,b_{pc}) = \left(\frac{0.80y+0.31Y}{0.83y+1.00b_{pc}}\right)b_c + \left(\frac{0.02b_{pc}-0.07Y}{0.75y+0.56b_{pc}}\right)b_{pc} \tag{34}$$

$$b_e = h(y,Y,b_c,b_{pc}) = \left(\frac{0.22y+0.38Y}{0.16y+0.31b_{pc}}\right)b_c + \left(\frac{0.05b_{pc}-0.16Y}{-0.03y+0.57b_{pc}}\right)b_{pc} \tag{35}$$

$$b_e = k(y,Y,b_c,b_{pc}) = \left(\frac{0.42y+0.11Y}{0.24y+0.90b_{pc}}\right)b_c + \left(\frac{0.11b_{pc}-0.08Y}{0.20y+1.00b_{pc}}\right)b_{pc} \tag{36}$$

Table 8. Accuracies of the Proposed Formula-based Approach

Soil covering depth	MAPE
(1) $Y > 2.4b_c$	5.1
(2) $2.4b_c > Y \geq 0$	30.4
(3) $0 > Y > -y$	34.2
(4) $Y \leq -y$	24.8
Average	28.9

Table 8 shows the prediction result of the proposed formula-based approach. In general, the result greatly improves the accuracy of the Melville and Coleman (2000) formula. The proposed method is able to simultaneously satisfy the requirements of accuracy and simplicity. The proposed formula has the advantages of being conceptually consistent with the observed scour behaviors and provides a solid scour depth prediction, which is an important and critical step in the bridge safety evaluation if floods are considered.

4. Conclusions

Taiwan is an elongated island with many rivers, and river bridges have become important traffic links. The pile group foundation is one of the main structures for bridges in Taiwan. However, establishing a practical approach to estimate the local scour depth for a pile group foundation has not drawn many attentions. Thus, a prediction formula of a relatively simple form with sufficient accuracy is preferred. To fulfill such target, experimental data of a total of 175 entries are collected to investigate accuracies of three available scour formulae, machine learning method and the proposed formula. Based on the analyses results, several important conclusions can be drawn as below.

1. The predictions of all three existing formulae do not provide satisfactory outcomes.
2. For the Melville and Coleman (2000) method, the equivalent width perpendicular to the flow (b_e) is a major source of error. On the other hand, $K_{h\,pier}$, suggested by HEC-18, fails to act like f/b_c when it is greater than 2.5.
3. The two LS-SVM models significantly improve the prediction performance and do not greatly vary from each other indicating that all scour contributing factors have been included in the two existing formulae of Melville & Coleman (2000) and HEC-18.
4. The results of the proposed formula, adopting the concept of the equivalent width, is able to significantly increase the prediction accuracy for most of conditions compared to the existing formulae.
5. The proposed formula-based approach has a similar format to that of the existing formulae, providing an analogous evaluation procedure without increasing the application difficulties.

Although there is still room for further refinement when the flow depth is lower than the pile-cap top for the proposed formula, the proposed formula has the advantages of being conceptually consistent with the observed scour behaviors and provides a satisfied scour depth prediction. Please note that the formula proposed was built using the collected experimental data, further validation is needed to generalize its use in future applications.

Acknowledgements

This study was supported by the TU-NTUST Joint Research Program. The support is gratefully acknowledged.

References

Andrić, J. M. and Lu, D. G. (2016). "Risk assessment of bridges under multiple hazards in operation period." *Safety Science*, Vol. 83, pp. 80-92, DOI: 10.1016/j.ssci.2015.11.001.

Arneson, L. A., Zevenbergen, L. W., Lagasse, P. F., and Clopper, P. E. (2012). *Evaluating scour at bridges*, Publication No. FHWA HIF 12-003, Federal Highway Administration, Washington, D.C.

Ataie-Ashtiani, B., Baratian-Ghorghi, Z., and Beheshti, A. A. (2010). "Experimental investigation of clear-water local scour of compound piers." *Journal of Hydraulic Engineering*, Vol. 136, No. 6, pp. 343-351, DOI: 10.1061/(ASCE)0733-9429(2010)136:6(343).

Azamathulla, H. M., Haghiabi, A. H., and Parsaie, A. (2016). "Prediction of side weir discharge coefficient by support vector machine technique." *Water Science and Technology: Water Supply*, Vol. 16, No. 4, pp. 1002-1016, DOI: 10.2166/ws.2016.014.

Bahrami, A., Monjezi, M., Goshtasbi, K., and Ghazvinian, A. (2011). "Prediction of rock fragmentation due to blasting using artificial neural network." *Engineering with Computers*, Vol. 27, No. 2, pp. 177-181, DOI: 10.1007/s00366-010-0187-5.

Cho, S. E. (2009). "Probabilistic stability analyses of slopes using the ANN-based response surface." *Computers and Geotechnics*, Vol. 36, No. 5, pp. 787-797, DOI: 10.1016/j.compgeo.2009.01.003.

Haghiabi, A. H., Azamathulla, H. M., and Parsaie, A. (2016). "Prediction of head loss on cascade weir using ANN and SVM." *ISH Journal of Hydraulic Engineering*, Vol. 1, No. 9, DOI: 10.1080/09715010.2016.1241724.

Hosseini, K., Karami, H., Hosseinjanzadeh, H., and Ardeshir, A. (2016). "Prediction of time-varying maximum scour depth around short abutments." *KSCE Journal of Civil Engineering*, Vol. 20, No. 5, pp. 2070-2081, DOI: 10.1007/s12205-015-0115-8.

Huang, C. L., Fan, J. C., Liao, K. W., and Lien, T. H. (2013). "A methodology to build a groutability formula via a heuristic algorithm." *KSCE Journal of Civil Engineering*, Vol. 17, No. 1, pp. 106-116, DOI: 10.1007/s12205-013-1847-y.

Imamoto H. and Ohtoshi K. (1987). "Local scour around a non-uniform circular pier." *Proceedings of IAHR Congress*, Lausanne, Switzerland, pp. 304-309.

Jain, S. C. and Ficher, E. E. (1980). "Sour around bridge piers at high flow velocities." *Journal of Hydraulic Engineering,* Vol. 106, pp. 1827-1842.

Khandelwal, M. (2011). "Blast-induced ground vibration prediction using support vector machine." *Engineering with Computers*, Vol. 27, No. 3, pp. 193-200, DOI: 10.1007/s00366-010-0190-x.

Kuo, Y. L., Jaksa, M. B., Lyamin, A. V., and Kaggwa, W. S. (2009). "ANN-based model for predicting the bearing capacity of strip footing on multi-layered cohesive soil." *Computers and Geotechnics*, Vol. 36, No. 3, pp. 503-516, DOI: 10.1016/j.compgeo.2008.07.002.

Lashkar-Ara, B., Ghotbi, S. M. H., and Najafi, L. (2016). "Prediction of scour in plunge pools below outlet bucket using artificial intelligence." *KSCE Journal of Civil Engineering*, Vol. 20, No. 7, pp. 2981-2990, DOI: 10.1007/s12205-016-1523-0.

Lee, J. J. and Kim, Y. S. (2010). "Development of advanced pattern recognition model for evaluation of lateral displacement on soft ground using support vector machine." *KSCE Journal of Civil Engineering*, Vol. 14, No. 2, pp. 173-182, DOI: 10.1007/s12205-010-0173-x.

Lewis, C.D. (1982). *Industrial and business forecasting methods*,

London, Butterworths.

Liao, K. W., Fan, J. C., and Huang, C. L. (2011). "An artificial neural network for groutability prediction of permeation grouting with microfine cement grouts." *Computers and Geotechnics*, Vol. 38, No. 8, pp. 378-386, DOI: 10.1016/j.compgeo.2011.07.008.

Liao, K. W. and Lee, Y. T. (2016). "Detection of rust defects on steel bridge coatings via digital image recognition." *Automation in Construction*, Vol. 71, No. 2, pp. 294-306, DOI: 10.1016/j.autcon.2016.08.008.

Melville, B. (2008). "The physics of local scour at bridge piers." *Proceedings of Fourth International Conference on Scour and Erosion*, Tokyo, Japan.

Melville, B. W. and Coleman, S. E. (2000). "Bridge scour." *Water Resources Publications*, Littleton, Colo.

Melville, B. W. and Raudkivi, A. J. (1996). "Effects of foundation geometry on bridge pier scour." *Journal of Hydraulic Engineering*, Vol. 122, No. 4, pp. 203-209, DOI: 10.1061/(ASCE)0733-9429(1996)122:4(203).

Najafzadeh, M. and Azamathulla, H. M. (2013). "Group method of data handling to predict scour depth around bridge piers." *Neural Computing & Applications*, Vol. 23, Nos. 7-8, pp. 2107-2112, DOI: 10.1007/s00521-012-1160-6.

Najafzadeh, M., Balf, M. R., and Rashedi, E. (2016). "Prediction of maximum scour depth around piers with debris accumulation using EPR, MT, and GEP models." *Journal of Hydroinformatics*, Vol. 18, No. 5, pp. 867-884, DOI: 10.2166/hydro.2016.212.

Parola, A. C., Mahavadi, S. K., Brown, B. M., and El-Khoury, A. (1996). "Effects of rectangular foundation geometry on local pier scour." *Journal of Hydraulic Engineering*, Vol. 122, No. 1, pp. 35-40, DOI: 10.1061/(ASCE)0733-9429(1996)122:1(35).

Raudkivi, A. J. (1986). "Functional trends of scour at bridge piers." *Journal of Hydraulic Engineering*, Vol. 112, No. 1, pp. 1-13, DOI: 10.1061/(ASCE)0733-9429(1986)112:1(1).

Raudkivi, A. J. and Ettema, R. (1983). "Clear-water scour at cylindrical piers." *Journal of Hydraulic Engineering*, Vol. 111, No. 4, pp. 713-731, DOI: 10.1061/(ASCE)0733-9429(1983)109:3(338).

Salim, M. and Jones, J. S. (1996). "Scour around exposed pile foundations." *North American Water and Environment Congress*, ASCE., Anaheim, U.S.A.

Suykens, J. A. K., Gestel, T. V., Brabanter, J. D., Moor, B. D., and Vandewalle, J. (2002). *Least Squares Support Vector Machines,* World Scientific Pub. Co. Singapore.

Wang, H., Tang, H., Liu, O., and Wang, Y. (2016). "Local scouring around twin bridge piers in open-channel flows." *Journal of Hydraulic Engineering,* Vol. 142, No. 9, pp. 06016008-1–6016008-8, DOI: 10.1061/(ASCE)HY.1943-7900.0001154.

Appendix. the Dataset used in This Study

y	b_c	b_{pc}	Lu	Y	V/V_c	d50 (10^{-3})	σ_g	d_s
0.20	0.05	0.08	0.04	0.11	1.00	0.80	1.00	0.10
0.20	0.03	0.08	0.05	0.04	1.00	0.80	1.00	0.04
0.60	0.03	0.12	0.05	0.03	0.75	0.47	1.30	0.08
0.30	0.15	0.21	0.06	0.15	1.18	1.00	1.00	0.34
0.20	0.01	0.08	0.07	0.02	1.00	0.80	1.00	0.02
0.20	0.03	0.08	0.06	0.20	1.00	0.80	1.00	0.06
0.20	0.05	0.06	0.01	0.05	1.00	0.80	1.00	0.10
0.60	0.03	0.12	0.05	-0.12	0.75	0.47	1.30	0.10
0.20	0.05	0.08	0.04	-0.20	1.00	0.80	1.00	0.16
0.15	0.02	0.09	0.15	-0.03	0.76	0.60	1.20	0.07
0.30	0.15	0.21	0.06	-0.03	1.18	1.00	1.00	0.14
0.20	0.05	0.06	0.01	-0.20	1.00	0.80	1.00	0.12
0.20	0.03	0.08	0.06	-0.04	1.00	0.80	1.00	0.11
0.22	0.06	0.37	2.78	0.00	0.82	0.80	1.00	0.04
0.33	0.10	0.19	0.05	-0.41	0.83	0.47	1.30	0.13
0.60	0.03	0.12	0.05	-0.67	0.75	0.47	1.30	0.07
0.14	0.02	0.09	0.15	-0.15	0.80	0.60	1.20	0.06
0.14	0.03	0.05	0.01	0.05	0.79	0.06	1.20	0.05
0.15	0.04	0.09	0.03	0.01	0.75	0.60	1.20	0.07
0.20	0.05	0.06	0.02	0.20	1.00	0.24	1.00	0.10
0.60	0.03	0.12	0.05	0.09	0.75	0.47	1.30	0.08
0.20	0.03	0.06	0.03	0.04	1.00	0.80	1.00	0.05
0.20	0.03	0.06	0.03	0.03	1.00	0.80	1.00	0.06
0.15	0.04	0.09	0.03	-0.02	0.78	0.60	1.20	0.08
0.15	0.02	0.09	0.15	0.00	0.84	0.60	1.20	0.02
0.30	0.15	0.30	0.15	0.00	1.18	1.00	1.00	0.18
0.15	0.03	0.05	0.01	0.00	0.79	0.06	1.20	0.05

0.30	0.15	0.21	0.06	0.00	1.18	1.00	1.00	0.17
0.20	0.05	0.06	0.02	-0.20	1.00	0.24	1.00	0.12
0.15	0.04	0.09	0.03	-0.02	0.78	0.60	1.20	0.09
0.15	0.04	0.09	0.03	-0.10	0.77	0.60	1.20	0.04
0.14	0.02	0.09	0.15	-0.18	0.76	0.60	1.20	0.05
0.15	0.04	0.09	0.03	-0.09	0.76	0.60	1.20	0.04
0.15	0.02	0.09	0.15	-0.11	0.79	0.60	1.20	0.06
0.30	0.15	0.30	0.15	0.03	1.18	1.00	1.00	0.25
0.20	0.03	0.08	0.06	0.02	1.00	0.80	1.00	0.06
0.20	0.05	0.06	0.02	0.09	1.00	0.24	1.00	0.10
0.33	0.10	0.19	0.05	0.21	0.83	0.47	1.30	0.21
0.20	0.05	0.06	0.02	0.06	1.00	0.80	1.00	0.10
0.15	0.04	0.09	0.03	0.04	0.75	0.60	1.20	0.06
0.20	0.05	0.06	0.02	0.08	1.00	0.24	1.00	0.09
0.15	0.04	0.09	0.03	-0.03	0.75	0.60	1.20	0.07
0.15	0.02	0.09	0.15	-0.01	0.76	0.60	1.20	0.04
0.26	0.06	0.37	2.78	0.00	0.70	0.80	1.00	0.04
0.30	0.15	0.30	0.15	-0.03	1.18	1.00	1.00	0.16
0.20	0.03	0.08	0.05	-0.05	1.00	0.80	1.00	0.11
0.15	0.02	0.09	0.15	-0.01	0.74	0.60	1.20	0.04
0.20	0.03	0.06	0.03	-0.20	1.00	0.80	1.00	0.13
0.20	0.01	0.08	0.07	-0.01	1.00	0.80	1.00	0.07
0.15	0.02	0.09	0.15	-0.16	0.72	0.60	1.20	0.04
0.15	0.02	0.09	0.15	-0.11	0.77	0.60	1.20	0.07
0.14	0.02	0.09	0.15	-0.16	0.79	0.60	1.20	0.06
0.30	0.15	0.30	0.15	0.15	1.18	1.00	1.00	0.24
0.20	0.03	0.08	0.05	0.03	1.00	0.80	1.00	0.04
0.15	0.02	0.09	0.15	0.01	0.79	0.60	1.20	0.02
0.20	0.03	0.06	0.03	0.20	1.00	0.80	1.00	0.07
0.33	0.10	0.19	0.05	0.16	0.83	0.47	1.30	0.18
0.15	0.02	0.09	0.15	0.04	0.79	0.60	1.20	0.04
0.14	0.04	0.09	0.03	0.01	0.80	0.60	1.20	0.05
0.15	0.04	0.09	0.03	-0.01	0.79	0.60	1.20	0.08
0.20	0.05	0.06	0.02	-0.20	1.00	0.80	1.00	0.13
0.15	0.03	0.05	0.01	-0.01	0.77	0.06	1.20	0.05
0.20	0.05	0.08	0.04	-0.06	1.00	0.80	1.00	0.14
0.60	0.03	0.12	0.05	-0.05	0.84	0.47	1.30	0.15
0.15	0.03	0.05	0.01	-0.03	0.78	0.06	1.20	0.07
0.15	0.02	0.09	0.15	-0.01	0.74	0.60	1.20	0.05
0.20	0.03	0.06	0.03	-0.06	1.00	0.80	1.00	0.11
0.14	0.04	0.09	0.03	-0.10	0.78	0.60	1.20	0.04
0.15	0.04	0.09	0.03	-0.07	0.77	0.60	1.20	0.04
0.15	0.04	0.09	0.03	-0.06	0.74	0.60	1.20	0.06
0.20	0.05	0.06	0.02	0.07	1.00	0.24	1.00	0.08
0.20	0.05	0.06	0.01	0.07	1.00	0.80	1.00	0.09
0.13	0.02	0.09	0.15	0.06	0.80	0.60	1.20	0.04
0.20	0.05	0.06	0.02	0.20	1.00	0.80	1.00	0.10
0.20	0.03	0.08	0.05	0.05	1.00	0.80	1.00	0.05
0.20	0.05	0.08	0.04	0.07	1.00	0.80	1.00	0.07
0.15	0.02	0.09	0.15	-0.01	0.79	0.60	1.20	0.05
0.20	0.03	0.08	0.05	-0.20	1.00	0.80	1.00	0.16
0.20	0.05	0.06	0.02	0.00	1.00	0.80	1.00	0.11
0.15	0.02	0.09	0.15	-0.02	0.85	0.60	1.20	0.06
0.20	0.03	0.08	0.06	-0.20	1.00	0.80	1.00	0.16
0.15	0.04	0.09	0.03	-0.02	0.77	0.60	1.20	0.08

0.20	0.03	0.08	0.06	0.00	1.00	0.80	1.00	0.08
0.26	0.06	0.37	2.78	0.00	0.91	0.80	1.00	0.08
0.15	0.02	0.09	0.15	-0.04	0.75	0.60	1.20	0.05
0.00	0.00	0.00	0.00	0.00	0.00	0.00	0.00	0.00
0.33	0.10	0.19	0.05	-0.11	0.83	0.47	1.30	0.19
0.20	0.05	0.06	0.02	0.05	1.00	0.24	1.00	0.09
0.33	0.10	0.19	0.05	0.05	0.83	0.47	1.30	0.21
0.15	0.03	0.05	0.01	0.01	0.77	0.06	1.20	0.03
0.20	0.03	0.08	0.05	0.03	1.00	0.80	1.00	0.07
0.20	0.05	0.08	0.04	0.20	1.00	0.80	1.00	0.10
0.15	0.03	0.05	0.01	0.06	0.76	0.06	1.20	0.05
0.15	0.04	0.09	0.03	0.02	0.80	0.60	1.20	0.04
0.15	0.02	0.09	0.15	-0.02	0.72	0.60	1.20	0.06
0.30	0.15	0.18	0.03	-0.03	1.18	1.00	1.00	0.12
0.20	0.05	0.06	0.02	0.00	1.00	0.24	1.00	0.11
0.20	0.01	0.08	0.07	-0.20	1.00	0.80	1.00	0.16
0.20	0.05	0.06	0.01	-0.07	1.00	0.80	1.00	0.11
0.24	0.06	0.37	2.78	0.00	0.53	0.80	1.00	0.03
0.15	0.02	0.09	0.15	-0.03	0.76	0.60	1.20	0.07
0.15	0.04	0.09	0.03	-0.10	0.74	0.60	1.20	0.04
0.33	0.10	0.19	0.05	-0.23	0.83	0.47	1.30	0.18
0.15	0.04	0.09	0.03	-0.07	0.78	0.60	1.20	0.05
0.20	0.05	0.06	0.02	0.07	1.00	0.80	1.00	0.09
0.20	0.05	0.06	0.02	0.03	1.00	0.24	1.00	0.10
0.20	0.01	0.08	0.07	0.01	1.00	0.80	1.00	0.01
0.20	0.05	0.08	0.04	0.06	1.00	0.80	1.00	0.08
0.14	0.02	0.09	0.15	0.07	0.76	0.60	1.20	0.04
0.20	0.03	0.08	0.05	0.20	1.00	0.80	1.00	0.07
0.20	0.03	0.08	0.06	0.03	1.00	0.80	1.00	0.03
0.15	0.02	0.09	0.15	-0.02	0.73	0.60	1.20	0.04
0.20	0.05	0.06	0.02	-0.06	1.00	0.80	1.00	0.12
0.60	0.03	0.12	0.05	-0.03	0.75	0.47	1.30	0.16
0.15	0.03	0.05	0.01	-0.01	0.79	0.06	1.20	0.06
0.15	0.02	0.09	0.15	-0.02	0.74	0.60	1.20	0.05
0.15	0.03	0.05	0.01	-0.02	0.78	0.06	1.20	0.06
0.14	0.02	0.09	0.15	0.00	0.84	0.60	1.20	0.03
0.60	0.03	0.12	0.05	-0.05	0.75	0.47	1.30	0.14
0.15	0.02	0.09	0.15	-0.05	0.75	0.60	1.20	0.05
0.15	0.02	0.09	0.15	-0.04	0.74	0.60	1.20	0.05
0.15	0.04	0.09	0.03	-0.06	0.79	0.60	1.20	0.05
0.30	0.15	0.18	0.03	0.03	1.18	1.00	1.00	0.17
0.20	0.01	0.08	0.07	0.20	1.00	0.80	1.00	0.02
0.20	0.03	0.06	0.03	0.05	1.00	0.80	1.00	0.05
0.20	0.03	0.08	0.05	0.06	1.00	0.80	1.00	0.06
0.20	0.05	0.06	0.02	0.06	1.00	0.24	1.00	0.08
0.20	0.05	0.06	0.01	0.20	1.00	0.80	1.00	0.10
0.20	0.05	0.06	0.02	0.05	1.00	0.24	1.00	0.09
0.15	0.03	0.05	0.01	-0.02	0.78	0.06	1.20	0.06
0.20	0.01	0.08	0.07	0.00	1.00	0.80	1.00	0.05
0.20	0.05	0.08	0.04	0.00	1.00	0.80	1.00	0.11
0.15	0.04	0.09	0.03	0.00	0.76	0.60	1.20	0.09
0.20	0.03	0.06	0.03	0.00	1.00	0.80	1.00	0.08
0.33	0.10	0.19	0.05	-0.10	0.83	0.47	1.30	0.20
0.33	0.10	0.19	0.05	-0.05	0.83	0.47	1.30	0.23
0.20	0.01	0.08	0.07	-0.05	1.00	0.80	1.00	0.10

0.15	0.04	0.09	0.03	-0.07	0.75	0.60	1.20	0.06
0.15	0.02	0.09	0.15	-0.12	0.78	0.60	1.20	0.06
0.15	0.02	0.09	0.15	-0.04	0.75	0.60	1.20	0.06
0.20	0.01	0.08	0.07	0.02	1.00	0.80	1.00	0.02
0.15	0.02	0.09	0.15	0.00	0.76	0.60	1.20	0.01
0.30	0.15	0.21	0.06	0.03	1.18	1.00	1.00	0.22
0.20	0.03	0.08	0.06	0.03	1.00	0.80	1.00	0.03
0.20	0.05	0.08	0.04	0.09	1.00	0.80	1.00	0.10
0.20	0.03	0.06	0.03	0.03	1.00	0.80	1.00	0.06
0.15	0.04	0.09	0.03	0.05	0.75	0.60	1.20	0.06
0.15	0.02	0.09	0.15	-0.01	0.74	0.60	1.20	0.03
0.15	0.03	0.05	0.01	-0.01	0.79	0.06	1.20	0.07
0.20	0.05	0.06	0.01	0.00	1.00	0.80	1.00	0.10
0.15	0.02	0.09	0.15	-0.02	0.76	0.60	1.20	0.06
0.16	0.02	0.09	0.15	0.00	0.75	0.60	1.20	0.03
0.20	0.03	0.08	0.05	0.00	1.00	0.80	1.00	0.09
0.15	0.04	0.09	0.03	-0.01	0.78	0.60	1.20	0.09
0.15	0.02	0.09	0.15	-0.01	0.76	0.60	1.20	0.05
0.14	0.02	0.09	0.15	-0.07	0.80	0.60	1.20	0.07
0.14	0.02	0.09	0.15	-0.18	0.77	0.60	1.20	0.05
0.33	0.10	0.19	0.05	-0.16	0.83	0.47	1.30	0.18
0.33	0.10	0.19	0.05	0.08	0.83	0.47	1.30	0.18
0.13	0.02	0.09	0.15	0.05	0.81	0.60	1.20	0.04
0.20	0.05	0.08	0.04	0.04	1.00	0.80	1.00	0.09
0.20	0.05	0.06	0.02	0.06	1.00	0.24	1.00	0.08
0.20	0.05	0.06	0.02	0.06	1.00	0.24	1.00	0.08
0.20	0.05	0.06	0.02	0.03	1.00	0.80	1.00	0.10
0.20	0.01	0.08	0.07	-0.03	1.00	0.80	1.00	0.09
0.60	0.03	0.12	0.05	0.00	0.75	0.47	1.30	0.15
0.60	0.03	0.12	0.05	-0.33	0.75	0.47	1.30	0.11
0.33	0.10	0.19	0.05	0.00	0.83	0.47	1.30	0.25
0.15	0.04	0.09	0.03	-0.03	0.76	0.60	1.20	0.07
0.15	0.02	0.09	0.15	-0.01	0.76	0.60	1.20	0.03
0.60	0.03	0.12	0.05	0.00	0.84	0.47	1.30	0.04
0.60	0.03	0.12	0.05	0.00	0.84	0.47	1.30	0.04
0.15	0.02	0.09	0.15	-0.17	0.77	0.60	1.20	0.06
0.60	0.03	0.12	0.05	-0.65	0.84	0.47	1.30	0.08
0.15	0.02	0.09	0.15	-0.16	0.79	0.60	1.20	0.06